The role of myosin 1c and myosin 1b for surfactant exocytosis

Nadine Kittelberger[1§], Markus Breunig[1§], René Martin[2], Hans-Joachim Knölker[2], Pika Miklavc[1,3]

[1] Department of General Physiology
University of Ulm
Albert-Einstein Allee 11
89081 Ulm
Germany

[2] Department of Chemistry
Technische Universität Dresden
Bergstr. 66
01069 Dresden
Germany

[3] to whom correspondence should be addressed
Department of General Physiology
University of Ulm
Albert-Einstein Allee 11
89081 Ulm
Germany
Tel. 49 731 500 23247
Fax. 49 731 500 23242
pika.miklavc@uni-ulm.de

[§] Nadine Kittelberger and Markus Breunig contributed equally to this work

Journal of Cell Science • Advance article

JCS Advance Online Article. Posted on 3 March 2016

Abstract

Actin and actin-associated proteins have a pivotal effect on regulated exocytosis in secretory cells and influence pre-fusion as well as post-fusion stages of exocytosis. Actin polymerization on secretory granules during the post-fusion phase (formation of an actin coat) is especially important in cells with large secretory vesicles or poorly soluble secretions. Alveolar type II (ATII) cells secrete hydrophobic lipo-protein surfactant, which does not easily diffuse from fused vesicles. Previous work showed that compression of actin coat is necessary for surfactant extrusion. Here we investigate the role of class 1 myosins as possible linkers between actin and membranes during exocytosis. Live cell microscopy showed translocation of fluorescently labelled myosin 1b and myosin 1c to the secretory vesicle membrane after fusion. Myosin 1c translocation was dependent on its pleckstrin homology (PH) domain. Expression of myosin 1b and myosin 1c constructs influenced vesicle compression rate, whereas only the inhibition of myosin 1c reduced exocytosis. These findings suggest that class 1 myosins participate in several stages of ATII cell exocytosis and link actin coats to the secretory vesicle membrane to influence vesicle compression.

Introduction

Exocytosis is a pivotal mechanism for secretion of mediators, transmitters and components of the extracellular space. The fusion of a secretory vesicle with the plasma membrane depends on a conserved group of proteins, which mediate the opening of the fusion pore (Fang and Lindau, 2014; Jahn and Fasshauer, 2012; Rizo and Südhof, 2012). Exocytosis is also influenced by actin and actin-associated proteins, which have inhibitory as well as stimulating roles in the pre-fusion and post-fusion phase of exocytosis (Eitzen, 2003; Malacombe et al., 2006; Papadopulos et al., 2013; Porat-Shliom et al., 2012). Although cortical actin network presents a barrier for vesicle fusion with the plasma membrane (Giner et al., 2005), actin fibers and associated motor proteins can facilitate vesicle transport to the site of exocytosis (Rojo Pulido et al., 2011). In addition, recent data obtained on cells with large secretory vesicles or poorly soluble secretions indicate that formation of the actin coat on fused vesicles has an important role in the post-fusion phase of exocytosis. Actin coat promotes compensatory endocytosis in oocytes (Sokac et al., 2003), stabilizes secretory vesicles in pancreatic acinar cells (Nemoto et al., 2004; Thorn, 2009), and provides the force for active content extrusion in endothelial cells (Nightingale et al., 2011; Nightingale et al., 2012), salivary gland cells (Masedunskas et al., 2011), and ATII cells (Miklavc et al., 2009; Miklavc et al., 2012; Miklavc et al., 2015). Several groups of myosin motor proteins associate with actin coats and influence its compression or organization (Masedunskas et al., 2011; Miklavc et al., 2012; Sokac et al., 2006; Yu and Bement, 2007).

Class 1 myosins function as linkers between membranes and actin cytoskeleton in several cellular processes. They have an N-terminal actin and nucleotide binding head domain, a calmodulin binding neck region, and a C-terminal membrane-binding tail domain (Barylko et al., 2005; McConnell and Tyska, 2010). The tail domain contains a pleckstrin homology (PH) domain, which enables direct association between myosin tail and acidic membrane lipids such as phosphatidyl inositol (4,5) bisphosphate (PIP_2) (Hokanson et al., 2006). Myosin 1 function is regulated by intracellular Ca^{2+} which binds to calmodulin and causes its dissociation from the neck domain (Lin et al., 2005; Manceva et al., 2007; Swanljung-Collins and Collins, 1991; Zhu et al., 1996). Of the eight known myosin 1 isoforms in vertebrates myosin 1a, 1c, and 1b are the best characterized (Greenberg and Ostap, 2013; McConnell and Tyska, 2010). Myosin 1a is expressed only in enterocytes, where it links actin bundles to the plasma membrane of brush border microvilli (Crawley et al., 2014). Myosin 1c influences numerous cellular processes, reaching from hair cell adaptation (Gillespie and Cyr, 2004; Stauffer et al., 2005), to

regulation of gene expression (Sarshad et al., 2013), G-actin transport during cell migration (Fan et al., 2012), and intracellular membrane trafficking (Bose et al., 2002; Bose et al., 2004; Brandstaetter et al., 2012; Chen et al., 2007; Sokac et al., 2006). Myosin 1c promotes insulin-dependent exocytosis of GLUT4-containing vesicles in muscle cells and adipocytes (Bose et al., 2002; Bose et al., 2004; Chen et al., 2007) and delivery of lipid raft associated proteins to the cell surface in HeLa cells (Brandstaetter et al., 2012). In *Xenopus* oocytes myosin 1c links actin coat to fused cortical granules and transduces force generated by actin coat to compress the vesicle membrane (Sokac et al., 2006). In contrast, myosin 1b colocalizes with endosomes (Raposo et al., 1999; Salas-Cortes et al., 2005) as well as with the plasma membrane (Komaba and Coluccio, 2010) and plays a role in generation of tubules from the Golgi network (Almeida et al., 2011; Coudrier and Almeida, 2011) and in ephrin signaling (Prosperi et al., 2015). Although myosin 1c and myosin 1b share structural similarities, their biophysical properties differ. Myosin 1c can generate force over a range of loads and was therefore suggested to play a role as a transport protein (Greenberg and Ostap, 2013; Greenberg et al., 2012). In contrast, myosin 1b is extremely sensitive to load and more likely functions as a force-sensitive anchor (Greenberg and Ostap, 2013; Laakso et al., 2008; Shuman et al., 2014).

Here we investigate the localization and function of myosin 1b and 1c during exocytosis of surfactant-containing secretory granules (lamellar bodies, LBs) in ATII cells. Surfactant is a hydrophobic material made of lipids and proteins, which inserts in the alveolar lining fluid to reduce surface tension and enable inspiration (Dietl and Haller, 2005; Dietl et al., 2004). The hydrophobicity of surfactant precludes simple diffusion from the fused vesicle and recent studies showed that actin coat formation on fused vesicles and its compression are pivotal for surfactant extrusion (Miklavc et al., 2012; Miklavc et al., 2015). In this study we show that both isoforms, myosin 1c and myosin 1b, translocate to fused LBs. However, their kinetics of translocation was strikingly different. Slow recruitment of myosin 1b to the vesicle membrane was likely due to an inhibitory effect of the motor activity in the head domain, whereas the translocation of myosin 1c depended on the intact PH domain in the tail region. Translocation of both isoforms was calcium sensitive. Myosin 1c inhibition reduced exocytosis and slowed down actin coat compression. In contrast, inactivation of the motor domain of myosin 1b enhanced the post-fusion vesicle compression.

Results

Endogenous expression of myosin 1 isoforms in ATII cells

To investigate the role of myosin 1 for ATII cell exocytosis, we first measured the relative expression of myosin 1 isoforms with RT-PCR (Fig. 1A). Myosin 1c, 1b and 1d had the highest expression rate in freshly isolated ATII cells as well as after 2 days of culture, whereas the lowest expression was detected for myosin 1a and 1g. In this work, we focus on localization and role of myosin 1b and myosin 1c during exocytosis in ATII cells as biophysical properties of both isoforms are well-characterized and commercial antibodies for immunostaining experiments on rat cells are available. In addition, myosin 1c was already described to participate in exocytosis (Bose et al., 2002; Sokac et al., 2006). Myosin 1b and 1c could be detected in ATII cells with western blot experiments (Fig. 1B) and on the membrane of fused LBs in immunostaining experiments, where the LB membrane was labelled by immunostaining of the ABCa3 lipid transporter, and fused vesicles were differentiated from non-fused vesicles by the presence of actin coats (phalloidin staining) (Fig. 1C).

Myosin 1b and myosin 1c translocation to the limiting membrane of secretory vesicles

We investigated the kinetics of myosin 1b and myosin 1c translocation to fused LBs by transfecting ATII cells with either myosin 1b-GFP or myosin 1c-GFP. The time point of LB fusion was determined with LysoTracker blue (LTB), which accumulates in LBs and diffuses in the extracellular space during exocytosis, resulting in a rapid decrease of fluorescent vesicle staining (Haller et al., 1998; Miklavc et al., 2012). Cells were co-transfected with actin-DsRed to detect actin coat formation on fused vesicles. Because the expression levels could influence the translocation kinetics, we compared the GFP fluorescence intensity of cells expressing different myosin 1 constructs using either fluorescence microscopy measurement on single cells or plate reader assay. There was no significant difference in GFP fluorescence between the myosin 1c or 1b wt and tail constructs (Suppl. Fig. 1). Myosin 1b-GFP and myosin 1c-GFP both translocated to LB membrane after fusion (Fig. 2). Translocation of myosin 1c-GFP to the vesicle membrane was significantly faster than the formation of the actin coat (half time of myosin 1c-GFP fluorescence increase on fused LBs calculated by one-phase association fit was 5.13 ± 0.9s, n=31 and half time of actin polymerization was 9.90 ± 1.26s, n=36; p=0.003; Fig. 2A,B). In contrast, myosin 1b-GFP translocation to the fused vesicles was significantly slower

than the actin coat formation (half time of myo1b-GFP fluorescence increase on fused LBs was 27.65 ± 3.14s, n=23; $p<0.0001$; Fig. 2C,D).

To investigate the reasons for the striking difference in the translocation kinetics of myosin 1c and myosin 1b we transfected the cells with GFP-coupled constructs containing only the membrane binding tail domains of myosin 1b or 1c (Fig. 3A). The half time of myosin 1c tail-GFP translocation to the vesicle membrane (5.11 ± 0.49s, n=24) was not significantly different from full-length myosin 1c, suggesting that the fast translocation of the full-length myosin 1c reflects the association of its tail domain with the vesicle membrane. In contrast, half time of myosin 1b tail-GFP fluorescence increase (8.67 ± 2.27s, n=14) was significantly shorter compared to the full-length myosin 1b-GFP ($p<0.0001$) and not significantly different from myosin 1c-GFP or myosin 1c tail-GFP. This observation indicates that the head domain may be responsible for the slow translocation of full-length myosin 1b to fused vesicles. To investigate whether the slow translocation was due to the motor activity of myosin 1b head domain, we inserted a R165A mutation in myosin 1b to block ATP hydrolysis and inactivate myosin 1b motor activity (Komaba and Coluccio, 2010; Shimada et al., 1997). The myosin 1b R165A-GFP mutant translocated to the fused LBs significantly faster than full-length myosin 1b-GFP (Fig. 3). Half time of myosin 1b R165A-GFP fluorescence intensity increase on fused LB (3.98 ± 0.71 s; n=10) was significantly shorter than the half time of wt myosin 1b-GFP translocation ($p<0.0001$, Mann-Whitney test; Fig. 3B) and not significantly different from myosin 1b tail-GFP. Myosin 1b R165A translocation was mostly transient (Fig. 3B) and in contrast to wt myosin 1b-GFP, which was recruited to vesicle membrane in all observed fusion events, only detectable on 75% of fused vesicles (n=24).

Both myosin 1 isoforms, 1b and 1c, were described to contain a PIP_2-binding PH domain in their tail region (Hokanson et al., 2006; Komaba and Coluccio, 2010), therefore we investigated the possibility that myosin 1b and 1c were recruited to fused LBs via PIP_2 in the LB membrane. To image PIP_2 localization in living cells we used a GFP-labelled PH domain of phospholipase Cδ (Czech, 2000; Várnai and Balla, 2007). PH-GFP was rapidly recruited to the LB membrane after fusion (half time 3.65 ± 0.49 s, n=22; Fig. 3C) indicating that PIP_2 was either translocated to or formed on the fused LBs. To detect PIP_2 together with myosin 1b or myosin 1c during LB exocytosis in the same cells we co-transfected the cells with PH-GFP and either myosin 1c-mCherry or myosin 1b-mCherry (Fig. 3D). The half time of PH-GFP fluorescence increase on fused vesicles was not significantly different from myosin 1c-mCherry and significantly shorter from myosin 1b-mCherry fluorescence increase ($p<0.001$). The remarkable similarity between the translocation kinetics of PH-GFP and myosin 1c-mCherry suggested that PH domain on the

tail of myosin 1c might determine myosin 1c translocation. To investigate this possibility, we transfected ATII cells with myosin 1c K892A-GFP and myosin 1c R903A-GFP constructs, where the mutations in the PH domain of myosin 1c tail region prevent PIP_2 binding (Hokanson et al., 2006). Both mutation-containing constructs localized to the cell cytoplasm and did not translocate to LB membrane after exocytosis (Fig. 3E), indicating the importance of the PH domain for myosin 1c translocation to the fused vesicles.

Irrespective of the lipids required for myosin 1b-GFP and myosin 1c-GFP attachment to the vesicle membrane, these isoforms could translocate to the vesicle membrane either by lateral diffusion from the plasma membrane into the vesicle membrane or they could be recruited from the cytosol. To investigate which possibility was more likely, we compared the recruitment of myosin 1b-GFP and myosin 1c-GFP to the fused vesicles with the recruitment of a GFP-coupled lyn-kinase membrane anchor domain. Lyn-GFP inserts into the inner leaflet of the plasma membrane with acyl anchors and translocates to the membrane of fused vesicles by lateral diffusion (Fig. 3G, (Miklavc et al., 2012)). The half time of wt myosin 1b-GFP translocation to the LB membrane was not significantly different from lyn-GFP (half time 29.29 ± 8.25s, n=10), whereas myosin 1c and myosin 1c tail constructs translocated to the vesicle membrane significantly faster than lyn-GFP (p<0.0001, Mann-Whitney test; Fig. 3H). To establish if the reason for this discrepancy lies in the different mobility of the constructs in the plane of the plasma membrane, we performed FRAP experiments. The half time of fluorescence recovery for lyn-GFP (4.94 ± 0.34s, n=31) was not significantly different from myosin 1c-GFP (6.22 ± 0.75s, n=29) or myosin 1c tail-GFP (4.28 ± 0.22s, n=32), suggesting that their mobility in the plasma membrane may be similar (Fig 3I). In contrast, fluorescence recovery half-time of myosin 1b-GFP (11.33 ± 1.63s, n=22) and myosin 1b tail-GFP (6.7 ± 0.41s, n=32) were significantly longer than lyn-GFP (p<0.0001 and p=0.002, respectively; Mann-Whitney test).

Calcium dependence of myosin 1b and 1c translocation to fused vesicles

Changes in cytoplasmic Ca^{2+} concentration influence myosin 1 motor activity (Greenberg and Ostap, 2013; McConnell and Tyska, 2010) and can also affect their binding to membranes directly (Tang et al., 2002) or by changing membrane properties (Hokanson and Ostap, 2006). To investigate the influence of calcium ions on myosin 1b and myosin 1c localization during ATII cell exocytosis, we applied calcium ionophore ionomycin or phorbol-12-myristate-13-acetate (PMA) to cells transfected with either myosin 1b-GFP or myosin 1c-GFP. Ionomycin causes a strong Ca^{2+} influx from the intracellular space, whereas PMA stimulates LB exocytosis

by directly activating protein kinase C and was used as control to elicit fusions without an increase in intracellular Ca^{2+} concentration (Frick et al., 2001). First, we determined whether the association of myosin 1b-GFP and myosin 1c-GFP with the plasma membrane is calcium dependent. We calculated the association of both constructs to the plasma membrane as a ratio between the fluorescence intensity at the edge of the cell and in the middle of the cell before and 300s after ionomycin or PMA stimulation (Fig. 4A, B) (Cai et al., 2013). The localization of myosin 1b and myosin 1c to the plasma membrane was confirmed by co-staining with membrane dye DiI (Suppl. Fig. 2). Ionomycin caused a significant decrease in fluorescence ratio for both myosin isoforms (from 0.55 ± 0.02 to 0.34 ± 0.02, n=32, $p<0.0001$ in myosin 1c and from 0.8 ± 0.06 to 0.21 ± 0.02, n=29, $p<0.0001$ in myosin 1b), which reflected the translocation from the plasma membrane to the cytosol upon Ca^{2+} elevation (Fig. 4C). PMA induced a small but significant decrease in membrane/cytosol ratio in myosin 1c transfected cells (0.6 ± 0.02 to 0.55 ± 0.02, n=33, $p=0.001$), whereas the difference in myosin 1b transfected cells was not significant (0.74 ± 0.06 before stimulation to 0.74 ± 0.06 after stimulation, n=25; Fig. 4C). The significance was calculated with the Wilcoxon matched-pairs signed rank test.

Because Ca^{2+} had such a profound influence on myosin 1c-GFP and myosin 1b-GFP association with the plasma membrane, we tested whether there is a difference in the post-fusion translocation of these constructs to the vesicle membrane. We measured translocation halftimes after ionomycin or PMA stimulation, and compared those with values after ATP stimulation, which is a physiological stimulus for LB exocytosis. In ATII cells ATP induces a transient general intracellular Ca^{2+} increase by stimulating Ca^{2+} release from the intracellular stores (Rooney, 2001), followed by a local perivesicular Ca^{2+} increase around fused vesicles (Miklavc et al., 2010; Miklavc et al., 2011). The half time of myosin 1c-GFP translocation to vesicle membrane after ionomycin stimulation was 8.90 ± 1.32 s (n=14), which was significantly longer than after PMA stimulation (5.10 ± 0.60 s, n=9; $p=0.04$) or after ATP stimulation (5.13 ± 0.9s, n=31; $p=0.02$; Fig.4D). A similar pattern was observed in myosin 1b-GFP transfected cells, where the translocation half time after ionomycin stimulation (42.03 ± 5.04s, n=9) was significantly longer than the half time of translocation after PMA stimulation (23.95 ± 2.97 s, n=8; $p=0.009$) and after ATP stimulation (27.65 ± 3.14s, n=23, $p=0.02$). The differences between ATP and PMA stimulation were not significant for both constructs (Fig. 4D).

Myosin 1 influence on exocytosis in ATII cells

After we have researched the possible causes for myosin 1b and 1c translocation to the fused LBs, we were interested in their function for LB exocytosis. It was already described that inhibition of myosin 1c has a negative effect on insulin-dependent exocytosis of GLUT4-containing vesicles in adipocytes (Bose et al., 2002; Bose et al., 2004) and skeletal muscle cells (Toyoda et al., 2011). We tested the influence of myosin 1c and 1b on exocytosis in ATII cells by expressing dominant negative myosin 1b tail or myosin 1c tail domain. The effect on exocytosis was determined by counting the number of cells, which responded to ATP stimulation with at least one fusion event (Fig. 5A). Transfection with myosin 1c tail-GFP reduced the proportion of responding cells (1.78±0.94%, n=12 independent experiments) compared to untransfected cells (5.58±0.54%, n=95 independent experiments; p=0.002), cells transfected with the wt myosin 1c-GFP (5.08±1.07%, n=26 independent experiments; p=0.04), or cells transfected with control construct lyn-GFP (4.21±0.92%, n=25 independent experiments; p=0.08). In contrast, transfection with myosin 1b tail-GFP did not affect exocytosis (5.24±1.44%, n=11 independent experiments). Up to 4 time lapse image sequences were analyzed for each experiment, up to 56 cells were analyzed for each image sequence. Mann-Whitney test was used for statistics.

In addition to genetic inhibition we used pharmacological inhibition with pentachloropseudilin (PClP), an allosteric inhibitor specific for class 1 myosins (Chinthalapudi et al., 2011; Martin et al., 2009). The percentage of responding ATII cells after 10 µM PClP treatment (0.29±0.2%, n=12 independent experiments) was significantly lower than the percentage of responding cells in untreated control cells (5.49±2%, n=11 independent experiments ~~44~~; p=0.0006, Mann-Whitney test; Fig. 5B). Up to 4 time lapse image sequences were analyzed for each experiment.

Myosin 1 coupling between actin coat and vesicle membrane

In addition to investigating the effect of dominant negative myosin 1b tail or myosin 1c tail constructs on the percentage of responding cells, we also investigated their effect on actin coating during the post-fusion phase of LB exocytosis. Transfection with dominant negative myosin 1b tail-GFP or myosin 1c tail-GFP did not inhibit actin coat formation (Fig. 6A). The half time of the actin coat polymerization in cells transfected with myosin 1b tail-GFP or myosin 1c tail-GFP was not significantly different from the half time in cells transfected with wt myosin 1b-GFP or wt myosin 1c-GFP or from cells expressing control GFP construct (Fig.

6B). In addition, transfection with tail domains of myo1c or myo1b constructs had no effect on the delay from fusion to actin coat formation (Fig. 6C). Inhibition of myosin 1 with PClP inhibitor also did not inhibit actin coats (Suppl. Fig. 3).

Because the inhibition of myosin 1b and 1c had no obvious effect on actin coat formation we tested the hypothesis that the disruption of their function as a linker between actin coat and vesicle membrane may influence actin coat compression. The compression of fused vesicles in cells transfected with myosin 1b tail-GFP (measured as a decrease in vesicle diameter) was not significantly different from compression in cells transfected with the control construct lyn-GFP. Vesicle compression in cells transfected with full length myosin 1b-GFP was slower than in control cells, however the differences only reached significance at the time = 45s after fusion ($p = 0.01$; Fig. 6D). Interestingly, fused vesicles in cells co-transfected with myosin 1b R165A-GFP and actin-DsRed compressed significantly faster than vesicles in control cells which were transfected only with actin-DsRed (Fig. 6E). In contrast, vesicle compression was significantly reduced in cells transfected with dominant negative myosin 1c tail (Fig. 6F). Pharmacological inhibition of myosin 1 with PClP had an even stronger effect on the vesicle compression rate, as vesicles only compressed to 89,7% of initial vesicle diameter in PClP treated cells compared to 68.8% in lyn-GFP transfected cells (t=225s; Fig. 6F). In addition, we measured the compression of vesicles in cells co-transfected with myosin 1c-mCherry and PH-GFP to test for possible inhibitory effects of PH-GFP expression due to the binding of both constructs on PIP_2. The vesicle compression in cells co-expressing both constructs was slightly reduced compared to cells transfected with myosin 1c-mCherry alone and the differences were significant at time points 75 and 105s after fusion ($p = 0.03$ and $p = 0.01$; Fig. 6G).

Discussion

We showed previously that compression of actin coats on fused secretory vesicles in ATII cells is necessary for surfactant extrusion (Miklavc et al., 2012). The actin coat compresses the fused vesicle by the combined action of myosin II and cofilin-mediated depolymerization of actin fibers followed by α-actinin-mediated cross-linking (Miklavc et al., 2015). Although we could identify Rho-GTPases and nucleation factors of the formin family as initiators of actin coat polymerization on fused LBs (Miklavc et al., 2012), the mechanisms of actin coat attachment to the vesicle membrane are not clear. In this work we demonstrate that myosin 1b and myosin 1c translocate to the membrane of fused secretory vesicles in ATII cells and that their inhibition influences the compression of actin coat. In addition, inhibition of myosin 1c also reduces exocytosis in ATII cells, suggesting that myosin 1 family can play a role in several stages of surfactant exocytosis.

Myosin 1 family members attach actin cytoskeleton to membranes (Barylko et al., 2005; Coudrier and Almeida, 2011; Laakso et al., 2008; McConnell and Tyska, 2010) and were suggested to play a role in several stages of secretory process (Bond et al., 2011; Woolner and Bement, 2009). Myosin 1c couples actin coat to the membrane of fused vesicles in oocytes (Sokac et al., 2006). The translocation of myosin 1c tail domain to the fused LBs suggests that tail domain alone is sufficient for translocation to fused vesicles, supporting the previously published observations (Hokanson et al., 2006; Sokac et al., 2006). Similarities in translocation kinetics of full length myosin 1c, myosin 1c tail or PH PLCδ to LBs suggest that myosin 1c translocation to fused vesicles is PIP2 dependent. Mutation of the basic residues in the PH domain (K892A and R903A), which prevent myo1c binding to PIP_2 lipids (Hokanson et al., 2006), completely abolished translocation of myo1c to the LB membrane after fusion.

Myo1b was previously shown to localize to endosomal compartments as well as to PIP_2-rich membrane regions (Komaba and Coluccio, 2010; Raposo et al., 1999; Ruppert et al., 1995) and its association with actin coats on fused vesicles was so far not described. Sequence similarities between the myo1c and myo1b PH domain suggested similar lipid binding properties (Hokanson et al., 2006). Although in ATII cells the half time of myo1b tail translocation to fused LBs was not significantly different from the translocation of myo1c or myo1c tail domain, the translocation of full-length myo1b to the vesicle membrane was significantly slower. This is consistent with previous observations (Mazerik et al., 2014), where single molecule total internal reflection fluorescence microscopy showed reduced mobility of full length myo1b in

the plasma membrane. FRAP experiments in ATII cells showed slower diffusion of myo1b in the plane of the plasma membrane compared to myo1c or the control construct lyn-GFP. In addition, ATP hydrolysis deficient myo1b R165A mutant translocated to the fused vesicles significantly faster than the wt myo1b suggesting that actin-binding head domain may be involved in retention of myo1b at the membrane of fused vesicles.

The full-length myo1b translocated to the vesicle membrane with a similar kinetics as lyn-GFP, which is inserted in the inner leaflet of the plasma membrane by the myristyl and palmityl anchors (Kovárová et al., 2001). Although slow translocation of full-length myo1b to the secretory vesicles after fusion may be explained by its actin binding as discussed above, the equally slow translocation of lyn-GFP cannot be explained in this way. FRAP experiments suggest that mobility of lyn-GFP is comparable to the mobility of myo1c and myo1c tail constructs, which is consistent with reports on fast diffusion of lyn-GFP in the plane of the plasma membrane (Schmidt and Nichols, 2004). It is therefore possible that the rapid translocation of full-length myo1c and myo1c tail to the fused vesicles is due to the recruitment of myosin 1 from the cytosol. Alternatively, the fusion pore structure may represent a barrier for lateral diffusion of membrane proteins with lipid anchors.

Cytosolic calcium plays an important role for surfactant secretion. The increase in intracellular calcium concentration caused by cell stretch or extracellular ATP are the most potent physiological stimuli leading to LB exocytosis (Dietl et al., 2010; Dietl et al., 2012) and widening of the fusion pore. (Miklavc et al., 2011). Motor activity and membrane binding properties of myosin 1 depend on the cytoplasmic calcium concentration (Greenberg and Ostap, 2013; McConnell and Tyska, 2010; Tang et al., 2002) and it is therefore possible that changes in Ca^{2+} concentration during exocytosis in ATII cells may influence myosin 1 translocation to the secretory vesicles as well as its function. Calcium binding changes myosin 1 force generation capability (Lin et al., 2005; Swanljung-Collins and Collins, 1991; Zhu et al., 1996) and was also suggested to promote membrane attachment (Cyr et al., 2002; Swanljung-Collins and Collins, 1992). In contrast, elevation of intracellular Ca^{2+} concentration by ionomycin in HEK cells caused the translocation of the myo1c tail domain from the plasma membrane to the cytosol (Hokanson and Ostap, 2006). Our findings in ATII cells also suggest that Ca^{2+} elevation does not promote membrane binding. Addition of ionomycin resulted in a marked translocation of myo1c and myo1b from the plasma membrane to the cytosol. Stimulation with PMA had no effect on myo1b translocation. However, it caused a small but significant translocation of myo1c from the plasma membrane to the cytosol. This observation may be due to the direct effect of the PMA on the decrease of PIP_2 concentration on the plasma membrane (Zeng et al.,

2003), which may affect myo1c more strongly as myo1b. The translocation to the membrane of fused vesicles was slower after ionomycin stimulation compared to PMA stimulation for both constructs, myo1b and myo1c. Interestingly, the translocation half times after ATP and PMA stimulation were not significantly different. This may be explained by the transient Ca2+ increase after ATP stimulation versus prolonged cell fusion response.

Myosin 1b and myosin 1c translocated to the fused secretory vesicles after fusion pore opening, which suggests that their main function may be during the post-fusion phase of exocytosis. We did not find significant differences in actin coat polymerization when we compared half times of actin polymerization and the delay between fusion and the start of actin coat formation after myo1b/myo1c inhibition. This suggests that myo1b and myo1c likely do not play a major role in actin coat formation. However, our results suggest that myo1b and 1c may be necessary for the normal coat compression. In oocytes uncoupling of actin coat from the vesicle membrane by transfecting cells with myo1c-tail resulted in inhibition of coat compression (Sokac et al., 2006). We could confirm this observation in ATII cells. Interestingly, although the transfection of cells with the myo1b tail had no effect on vesicle compression, we observed a marked increase in the vesicle compression rate after transfecting the cells with the myo1b R165A mutant. Conversely, overexpression of wt myo1b resulted in slight decrease in vesicle compression rate. These observations suggests that myo1b might play a role of a tension sensitive "anchor" for the vesicle compression as suggested by biophysical properties of myo1b (Laakso et al., 2008; Laakso et al., 2010). PClP, an allosteric inhibitor which reversibly binds near actin binding region on the myosin motor domain was shown to be specific for myosin 1 family, and inhibits myo1c as well as myo1b (Chinthalapudi et al., 2011; Martin et al., 2009). We observed that PC1P treatment decreased the rate of vesicle compression without affecting actin coat formation similar to genetic inhibition of myosin 1c. This might be due to higher expression of myo1c in ATII cells or to a more notable physiological role of myo1c in actin coat compression compared to myo1b. A similar observation was made in HeLa cells, where PClP inhibition resulted in identical changes in lysosomal morphology as described in siRNA knock-down of myo1c (Chinthalapudi et al., 2011).

Myo1c was not only reported to connect actin coat to the membrane of fusing vesicles but also to facilitate vesicle fusion with the plasma membrane. In adipocytes and skeletal muscle cells myo1c inhibition leads to a decreased exocytosis of GLUT4-containing vesicles after insulin stimulation (Bose et al., 2002; Bose et al., 2004; Toyoda et al., 2011) and in HeLa cells to decreased incorporation of GPI-linked proteins in the plasma membrane (Brandstaetter et al., 2012). TIRF experiments showed that myo1c tethers GLUT4 vesicles to the plasma membrane

and the absence of this tethering inhibits exocytosis (Boguslavsky et al., 2012). It is not yet clear whether myo1c promotes LB exocytosis in ATII cells via the same tethering mechanism. However, it is more likely that the function of myo1c is in cortical actin rearrangement or LB tethering to the plasma membrane than in active vesicular transport. Although the proteomics study on isolated LBs suggested that there are myo1c as well as myo1b molecules associated with LBs (Ridsdale et al., 2011), we could observe a strong translocation of myo1c and myo1b to LB membrane only after fusion while their presence on non-fused LBs was not detectable by conventional fluorescence microscopy.

Together these data indicate that myo1c and myo1b translocate to secretory vesicles in ATII cells after fusion. The translocation of myo1c to the vesicle membrane closely resembled the translocation of PH-PLCδ, whereas the translocation of myo1b was markedly slower. The inhibition of myosin 1c reduced secretory vesicle exocytosis and slowed down actin coat compression. In contrast, myosin 1b R165A induced an increase in actin coat compression rate, suggesting that several mechanisms are necessary for efficient actin coat compression.

Material and Methods

Cell isolation and transfection

ATII cells were isolated from the lungs of male Sprague-Dawley rats, aged 3-4 months according to the procedure of Dobbs et al. (Dobbs et al., 1986) and cultured as recently described (Miklavc et al., 2010). Rats were kept at the central animal facility of the Ulm University according to guidelines for ethical care of animals. All experiments in this study were approved by the Regierungspräsidium Tübingen, Germany. Isolated cells were used for experiments for up to 48 h after isolation bec longer cell culture times result in rapid loss of ATII cell characteristics (Diglio and Kikkawa, 1977; Mason and Dobbs, 1980). ATII cells were transfected by electroporation or by adenoviral vectors as recently described (Miklavc et al., 2015).

Plasmids and adenoviral vectors

Plasmids expressing myosin 1c-GFP, myosin 1c tail-GFP, myosin 1c R903A-GFP and myosin 1c K892A-GFP were a kind gift from E. Michael Ostap (University of Pennsylvania, Philadelphia, USA) (Hokanson et al., 2006); myosin 1b-GFP and myosin 1b tail-GFP were generously provided by Evelyn Coudrier (Institut Curie, Paris, France) (Raposo et al., 1999), and PH-GFP adenovirus was kindly provided by Ora Weisz (University of Pittsburgh, Pittsburgh, USA) (Weixel et al., 2007). Myosin 1b R165A-GFP was created with Infusion system (Clontech, TakaraBio, France). Myosin 1c-mCherry was made by cloning PCR-amplified mCherry from pmCherry-N1 vector (Clontech, TakaraBio, France) in myosin 1c-GFP using *Age*I and *Not*I restriction sites. Myosin 1b-mCherry was made by cloning PCR-amplified mCherry from pmCherry-N1 vector (Clontech, TakaraBio, France) in myosin 1b-GFP using *Nhe*I and *Xho*I restriction sites. Adenoviruses expressing actin-GFP and actin-DsRed and plasmid for lyn-GFP were recently described (Frick et al., 2007; Miklavc et al., 2009; Miklavc et al., 2012). As control GFP plasmid we used pmax GFP^{TM} (Lonza, Germany).

Experimental conditions

For all experiments ATII cells were kept in bath solution (in mM: 140 NaCl, 5 KCl, 1 $MgCl_2$, 2 $CaCl_2$, 5 glucose, 10 Hepes; pH 7.4). Cells were stimulated for secretion with 100 µM ATP (Sigma, Schnelldorf, Germany), 300 nM PMA, or 3 µM ionomycin. Fusions were detected with LysoTracker Red (10 nM 10 min incubation) or Lysotracker Blue (100 nM, 20 min) (Haller et al., 1998). For pharmacological inhibition of myosin 1 ATII cells were preincubated with 10

µM PClP inhibitor for 2h. Fluorescent dyes were purchased from Molecular Probes (Life technologies, Darmstadt, Germany).

Semi-quantitative RT-PCR

RT-PCR was performed on 0.8-1.3µg RNA with SuperScript VILO synthesis kit and QuantiTect primer assays (Quiagen, Hilden, Germany) on a realplex2 mastercycler (Eppendorf, Hamburg, Germany) as described in detail previously (Miklavc et al., 2015).

Western blot analysis

Western blot was performed on freshly isolated ATII cells or ATII cells after 2 days of culture as described in detail earlier (Miklavc et al., 2011). Primary antibody against myosin 1c purchased from Abcam (catalogue number ab51261, lot number GR150630-3; Cambridge, UK) and primary antibody against myosin 1b purchased from Novus biologicals (catalogue number NBP1-87739, lot number A39461; Littleton, USA) were used in concentrations suggested by the manufacturer (1:1000 for myosin 1c and 1:500 for myosin 1b). Manufacturer verified antibody specificity.

Immunofluorescence

Primary antibody against ABCa3 was purchased from Abcam (catalogue number ab24751, lot number GR133811-2). Fluorescently labelled secondary antibodies and AlexaFluor Phalloidin 568 were purchased from Molecular Probes (Life technologies, Darmstadt, Germany). Immunofluorescence and image acquisition on Leica TCS SP5 microscope were performed as described earlier (Miklavc et al., 2015). We used primary antibody dilutions suggested by the manufacturer (1:50 for myosin 1b and 1c antibodies, 1:300 for ABCa3 antibody). Images were taken on Leica TCS SP5 confocal microscope (Leica, Wetzlar, Germany) using a 63x objective (Leica HCX PL APO lambda blue 63.0x1.40 OIL UV). Images for the green (AlexaFluor 488), red (AlexaFluor 568) and far red (AlexaFluor 647) channels were taken sequentially using appropriate excitation and emission settings.

Fluorescence imaging

Fluorescence imaging experiments on living cells were performed on an iMic digital microscope (Till Photonics, Gräfelfing, Germany) as described previously (Miklavc et al., 2015). FRAP experiments were performed on iMic microscope using green laser at 95% intensity to bleach a circular region of interest (diameter = 4 µm). DiI stained cells were imaged

on Cell Observer microscope (Visitron, Puchheim, Germany) with 40x oil immersion objective and MetaMorph acquisition software (Molecular devices, Sunnyvale, USA).

Image analysis and data presentation

Images were analysed using Fiji (NIH, Bethesda, USA). GraphPad Prism 5 (GraphPad Software, La Jolla, USA) was used for curve fitting and graph design. LB compression after fusion was analysed by measuring the vesicle perimeter at indicated time points after fusion. A circular region of interest was set around the fusing LB to determine the onset of LB fusion by measuring LysoTracker fluorescence or to measure the translocation of fluorescently labelled constructs (Miklavc et al., 2012; Miklavc et al., 2015). Figures were prepared with Adobe Photoshop CS2 (Adobe, San Jose, USA).

Statistical analysis

We used Excel (Microsoft, Redmond, USA) and GraphPad Prism 5 (GraphPad Software, La Jolla, USA) for statistical analysis. Unless stated otherwise, n indicates the number of fused vesicles where fluorescence changes were measured and was set to ≥5. The fusions were recorded in 4-21 independent experiments on ATII cells from 2-7 cell isolations. Only vesicles where fluorescence signal to noise ratio was sufficiently high and where the whole secretory process could be monitored were used for analysis (predefined). Unless stated otherwise data are presented as mean, SEM was used to estimate the variation within data groups (indicated for every data set) and two tailed t-test was used for statistical comparison. D'Agostino and Pearson omnibus normality test was used to estimate the data distribution.

Acknowledgements

We thank Paul Dietl and Edward Felder for helpful comments. Technical assistance by Tatiana Felder, Achim Riecker and Melanie Timmler and help with data analysis by M. Tabitha Müller are gratefully acknowledged.

Competing interests

The authors declare no competing or financial interests.

Author contributions

P.M. designed the study. N.K., M.B., and P.M. performed the experiments and analysed data. R.M. and H.-J.K. provided reagents. All authors wrote the manuscript.

Funding

This work was supported by grants from the Ministry of Science, Research and the Arts Baden-Württemberg to P.M. and by the Deutsche Forschungsgemeinschaft, grant D-1402/3-1.

Figures

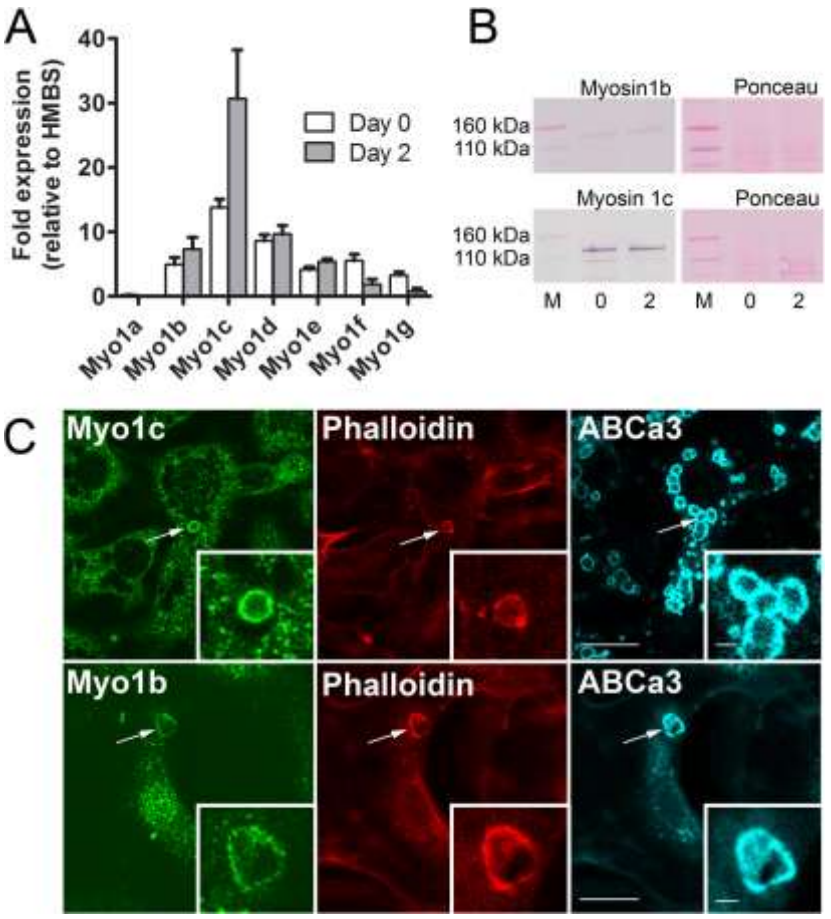

Figure 1: Expression and localization of myosin 1b and myosin 1c in ATII cells

A) RT-PCR showed that myosin 1b and 1c are among the highest expressed myosin 1 isoforms in ATII cells. Data (mean ± SEM) obtained from three cell isolations and three experiments per isolation are shown relative to the expression of the housekeeping gene *HMBS*.

B) Western blot of myosin 1b and 1c from freshly isolated ATII cells and ATII cells after 2 days of culture (0 and 2, respectively) to demonstrate expression of myosin 1b and 1c in ATII cells. Ponceau S staining was used to control for equal protein loading (M = marker).

C) Colocalization of anti myosin 1b and 1c antibodies with fused secretory vesicles marked by ABCa3 and phalloidin immunostaining. ABCa3 transporter is a marker for secretory vesicle membrane in ATII cells. After ATP stimulation some vesicles fused with the plasma membrane and acquired an actin coat, which was labeled by phalloidin staining. Scale bar = 10 µm. Inserts show the enlarged view of the fused LBs. Scale bar = 1 µm.

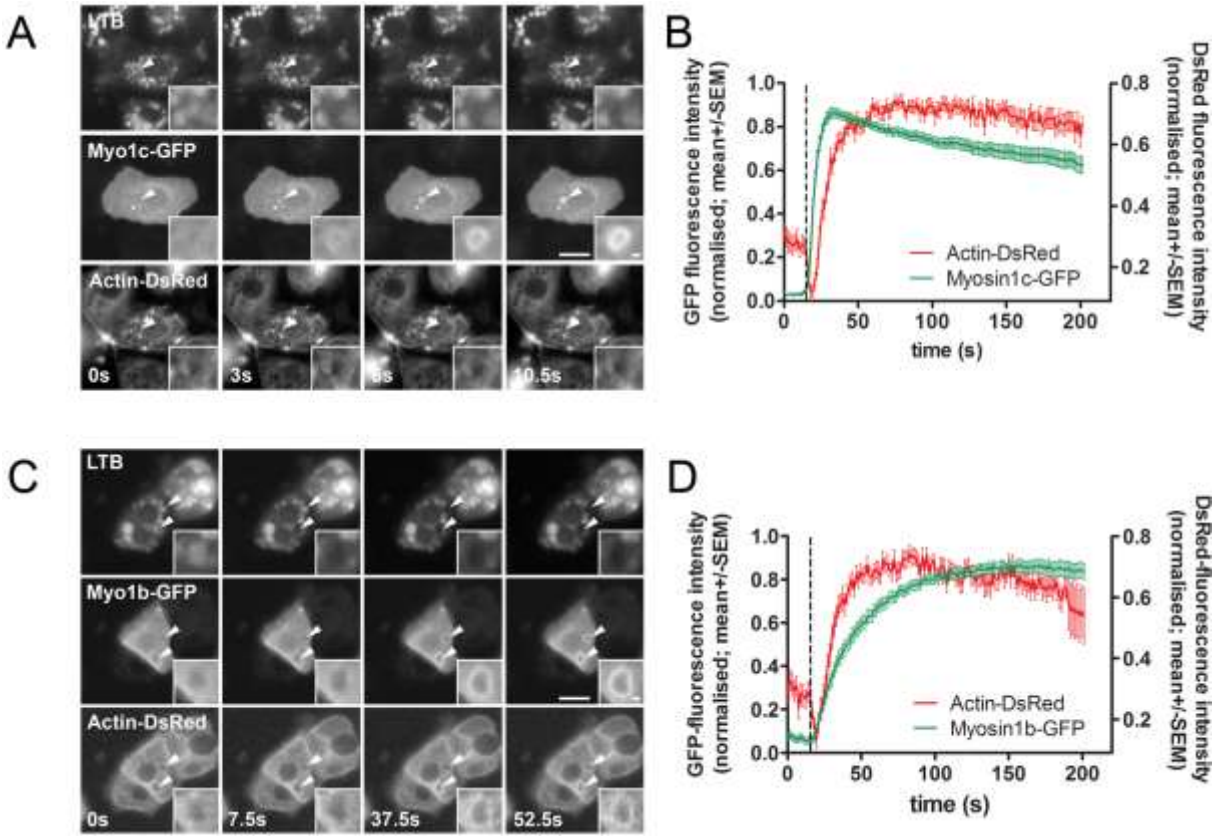

Figure 2: Translocation of myosin 1b-GFP and myosin 1c-GFP to fused secretory vesicles.

A) ATII cells were co-transfected with myosin 1c-GFP and actin-DsRed and stained with LTB. Myosin 1c-GFP translocated to secretory vesicles after fusion. Arrowheads indicate fusing vesicles and time=0 indicates the last frame before fusion. Scale bar = 10 µm. The time of fusion pore opening was determined by LTB fluorescence decrease (upper row). Inserts show the enlarged view of the fused vesicle (scale bar = 1 µm).

B) Mean ± SEM of the myosin 1c-GFP and actin-DsRed fluorescence change on fusing LBs (n=31). Myosin 1c-GFP translocated to fused vesicles before actin polymerization. The dashed line indicates the last frame before the fusion pore opening, determined by LTB fluorescence decrease.

C) ATII cells were co-transfected with myosin 1b-GFP and actin-DsRed and stained with LTB. Myosin 1b-GFP translocated to secretory vesicles after fusion. Arrowheads point at fusing LBs and time=0 indicates the last frame before the fusion pore opening. Scale bar = 10 µm. The time of fusion pore opening was determined by LTB fluorescence decrease (upper row). Inserts show the enlarged view of one fusing vesicle (scale bar = 1 µm).

D) Mean ± SEM of the myosin 1b-GFP and actin-DsRed fluorescence change on the fusing LBs (n=42). The kinetics of myosin 1b-GFP translocation was slower than actin polymerization and also slower than myosin 1c translocation (Fig. 2B). The dashed line indicates the last frame before the fusion pore opening.

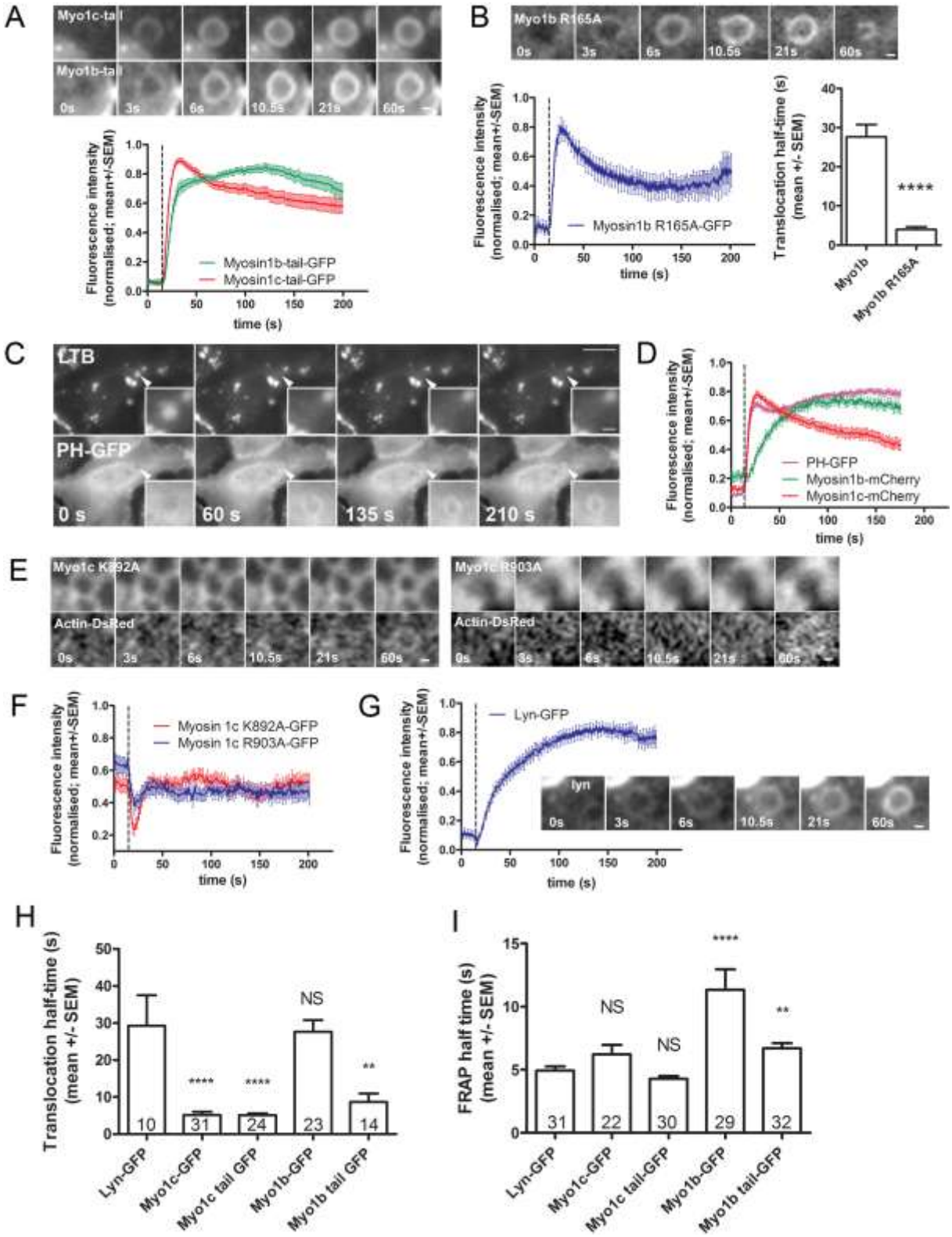

Figure 3: Kinetics of myosin 1b and myosin 1c translocation to fused vesicles.

A) The image series shows single fusing vesicles in myosin 1b tail-GFP or myosin 1c tail-GFP transfected ATII cells. Myosin 1b tail-GFP and myosin 1c tail-GFP translocated to fused

secretory vesicles. Time=0 indicates the last frame before the fusion pore opening, scale bar = 1 µm. The graph shows the mean ± SEM of the myosin 1b tail-GFP and myosin 1c tail-GFP fluorescence increase on fused LBs (n=28 and 38, respectively). Both tail domains translocated to the fused secretory vesicles with similar kinetics. The dashed line indicates the last frame before the fusion pore opening.

B) Myosin 1b R165A-GFP translocated to fused vesicles with faster kinetics than myosin 1b-GFP (see Fig. 2D). The image series shows single fusing vesicle in ATII cell transfected with myosin 1b R165A-GFP (Scale bar = 1 µm). The graphs show the mean ± SEM of the myosin 1b R165A-GFP fluorescence change on the site of the fused LBs (n=18, left) and the comparison of the half times of myosin 1b-GFP and myosin 1b R165A-GFP fluorescence increase on fused vesicles (n=23 and 10, respectively; right). The dashed line on the graph and time = 0 s on the image series indicate the last frame before the fusion pore opening. The half time of myosin 1b R165A-GFP was significantly shorter compared to full-length myo1b-GFP (**** $p<0.0001$, two-tailed Mann-Whitney test).

C) ATII cell transfected with PH-GFP and stained with LTB. Arrowhead points at the fusing LB and the inserts show the enlarged view of the fused vesicle. PH-GFP translocated to secretory vesicles after fusion (bottom row). The time of fusion pore opening was determined by LTB fluorescence decrease (upper row). Time=0 indicates the last frame before the fusion pore opening. Scale bars: 10 µm (image) and 1 µm (insert).

D) Mean ± SEM of PH-GFP, myosin 1b-mCherry, and myosin 1c-mCherry fluorescence increase on the fused LBs (n=97, 36, and 61, respectively). The dashed line indicates the last frame before the fusion pore opening, determined by LTB fluorescence decrease. Note the similar kinetics of LB localization in PH-GFP and myosin 1c-mCherry and the slower translocation of myosin 1b-mCherry.

E) Single fusing vesicles in ATII cells transfected with GFP-coupled myosin 1c constructs with a PH-domain mutation R903A or K892A and co-transfected with actin-DsRed. These constructs had cytoplasmic localization and did not translocate to fused vesicles after fusion. The GFP fluorescence (above) and DsRed fluorescence (below) are shown for each vesicle. Time=0 indicates the last frame before the fusion pore opening, scale bar = 1 µm.

F) Mean ± SEM of the myosin 1c K892A-GFP and myosin 1c R903A-GFP fluorescence change on the site of the fused LBs (n=34 and 30, respectively). No translocation of myosin 1c K892A-GFP and myosin 1c R903A-GFP to secretory vesicles could be observed after fusion. Fusion pore opening is indicated by the dashed line.

G) Mean ± SEM of the lyn-GFP fluorescence increase on fused LBs (n=20) and an image sequence of a single fusing vesicle in a lyn-GFP transfected ATII cell. Lyn-GFP translocated to fused vesicles with relatively slow kinetics compared to myosin 1c-GFP or PH-GFP. The dashed line on the graph and t = 0 s on the image sequence indicate the last frame before the fusion pore opening. Scale bar = 1 µm.

H) Translocation half times of GFP-tagged myosin 1b and myosin 1c constructs compared to lyn-GFP. The translocation of myosin 1b-GFP to the membrane of fused vesicles was not significantly different from lyn-GFP, whereas the translocation of other tested constructs was significantly faster (n = number of vesicles, ** $p<0.01$, **** $p<0.0001$, NS=not significant; two-tailed Mann-Whitney test).

I) Half times of fluorescence recovery after photobleaching for the same constructs shown on Fig. 3H. The bleaching area (diameter = 4 µm) was chosen on the edge of the cell and fluorescence recovery was measured in 0.5s intervals. The FRAP half-time of lyn-GFP was not significantly different from the myosin 1c-GFP and myosin 1c tail-GFP constructs, whereas the FRAP half-time was markedly prolonged in myosin 1b-GFP (n = number of cells where FRAP was performed; ** $p<0.05$, **** $p<0.0001$, NS=not significant; two-tailed Mann-Whitney test).

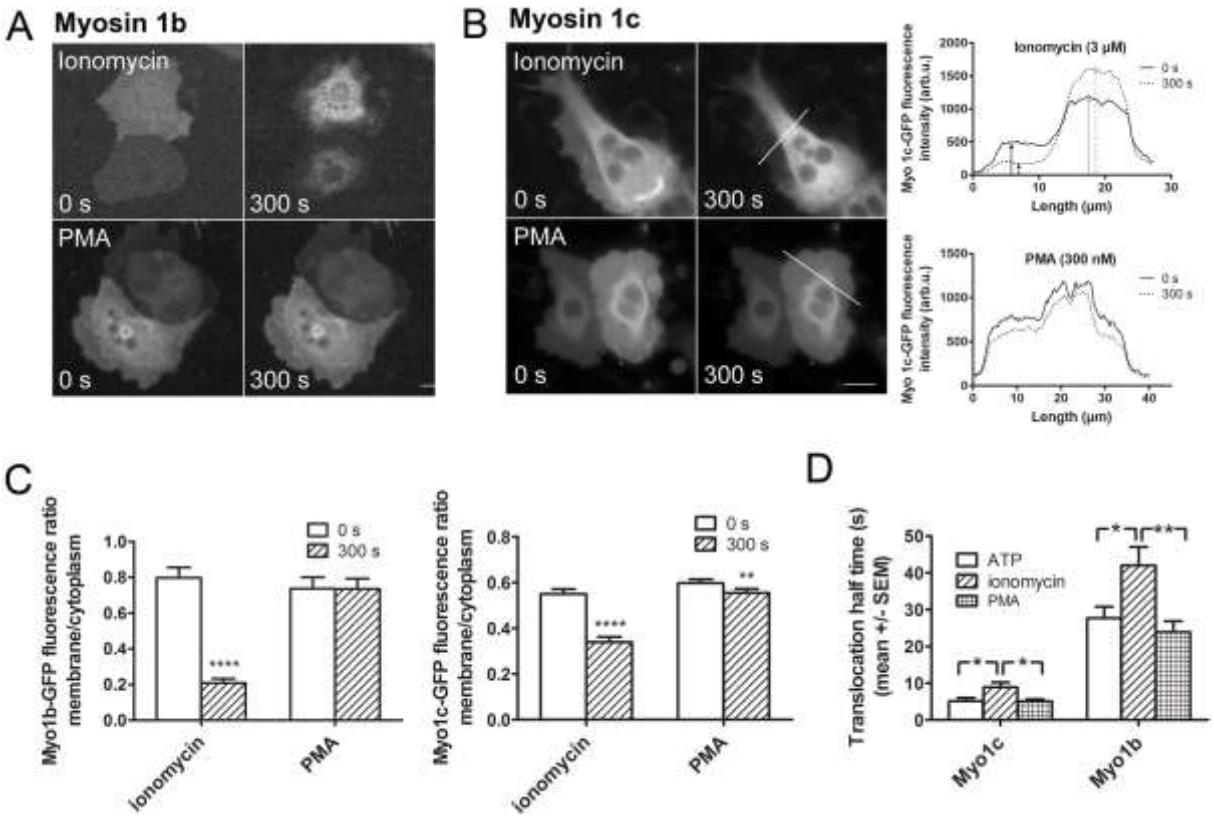

Figure 4: Ca^{2+} dependency of myosin 1b and myosin 1c translocation.

A) Myosin 1b-GFP transfected ATII cells before (time = 0 s) and after (300 s) stimulation with either ionomycin (upper row) or PMA (bottom row). A change in myosin 1b localization was only observed after ionomycin stimulation. Scale bar = 10 µm.

B) Myosin 1c-GFP transfected ATII cells (left) before (time = 0 s) and after (300 s) stimulation with either ionomycin (upper row) or PMA (bottom row). Scale bar = 10 µm. The lines on the right side indicate the location of the line scan measurement. Line scans were used to calculate ratio between the fluorescence intensity of the edge of the cell (black arrows) and the center of the cell (grey arrows), before (solid line) and 300 s after stimulation (dashed line).

C) Comparison of the fluorescence ratio between the cell membrane and the cell cytoplasm for ionomycin or PMA stimulation in ATII cells transfected with either myosin 1b-GFP (left graph) or myosin 1c-GFP (right graph). The fluorescence ratio membrane/cytoplasm of myosin 1b-GFP and myosin 1c-GFP decreased significantly after ionomycin stimulation, whereas PMA stimulation only affected myosin 1c localization. N=29 and 25 cells transfected with myosin 1b-GFP, and 32 and 33 cells transfected with myosin 1c-GFP for ionomycin and PMA

stimulation, respectively (** $p<0.01$, **** $p<0.0001$, two-tailed Wilcoxon matched-pairs signed rank test).

D) Half times of myosin 1c-GFP and myosin 1b-GFP translocation to fused vesicles after cell stimulation with either ATP, ionomycin or PMA. After ionomycin stimulation the translocation of both myosin isoforms, myosin 1b-GFP and myosin 1c-GFP was significantly slower than after PMA or ATP stimulation. N=31, 14, and 9 vesicles in myosin 1c-GFP transfected cells, and 23, 9, and 8 vesicles in myosin 1b-GFP transfected cells for ATP, ionomycin and PMA stimulation, respectively (*$p<0.05$; **$p<0.01$; two-tailed t-test).

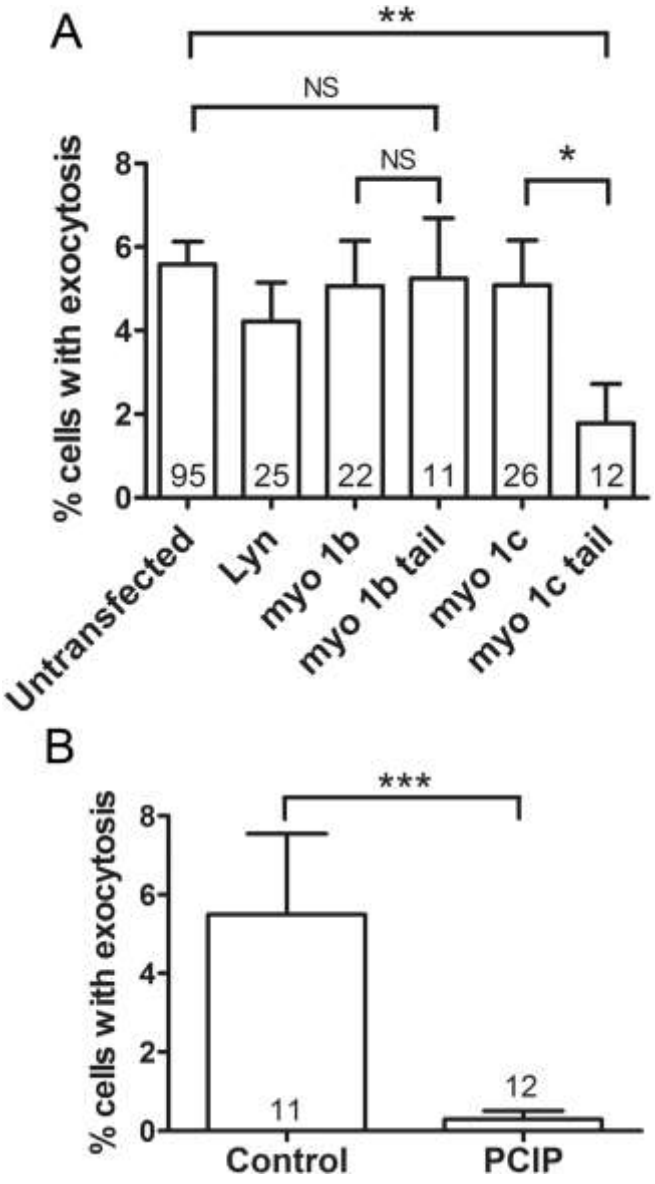

Figure 5: The influence of myosin 1c and myosin 1b on exocytosis

A) The proportion of cells responding to ATP stimulation with exocytosis in untransfected ATII cells and in cells transfected with lyn-GFP control construct or myosin 1b/myosin 1c constructs. The percentage of cells with exocytosis was significantly reduced in cells transfected with myosin 1c tail-GFP compared to untransfected cells and full-length myosin 1c-GFP. Transfection with myosin 1b tail-GFP did not significantly change the proportion of cells with exocytosis. Numbers indicate the number of independent experiments, up to 4 time-lapse image sequences were analyzed for each experiment, up to 56 cells were analyzed for each image sequence (*p<0.05; **p<0.01; two-tailed Mann-Whitney test).

B) Incubation of ATII cells with 10 µM PClP inhibitor for 2 h significantly decreased the percentage of cells responding to ATP stimulation with exocytosis compared to untreated cells (***$p<0.001$; two-tailed Mann-Whitney test). Numbers indicate the number of independent experiments, up to 4 time-lapse image sequences were analyzed for each experiment, up to 36 cells were analyzed for each image sequence.

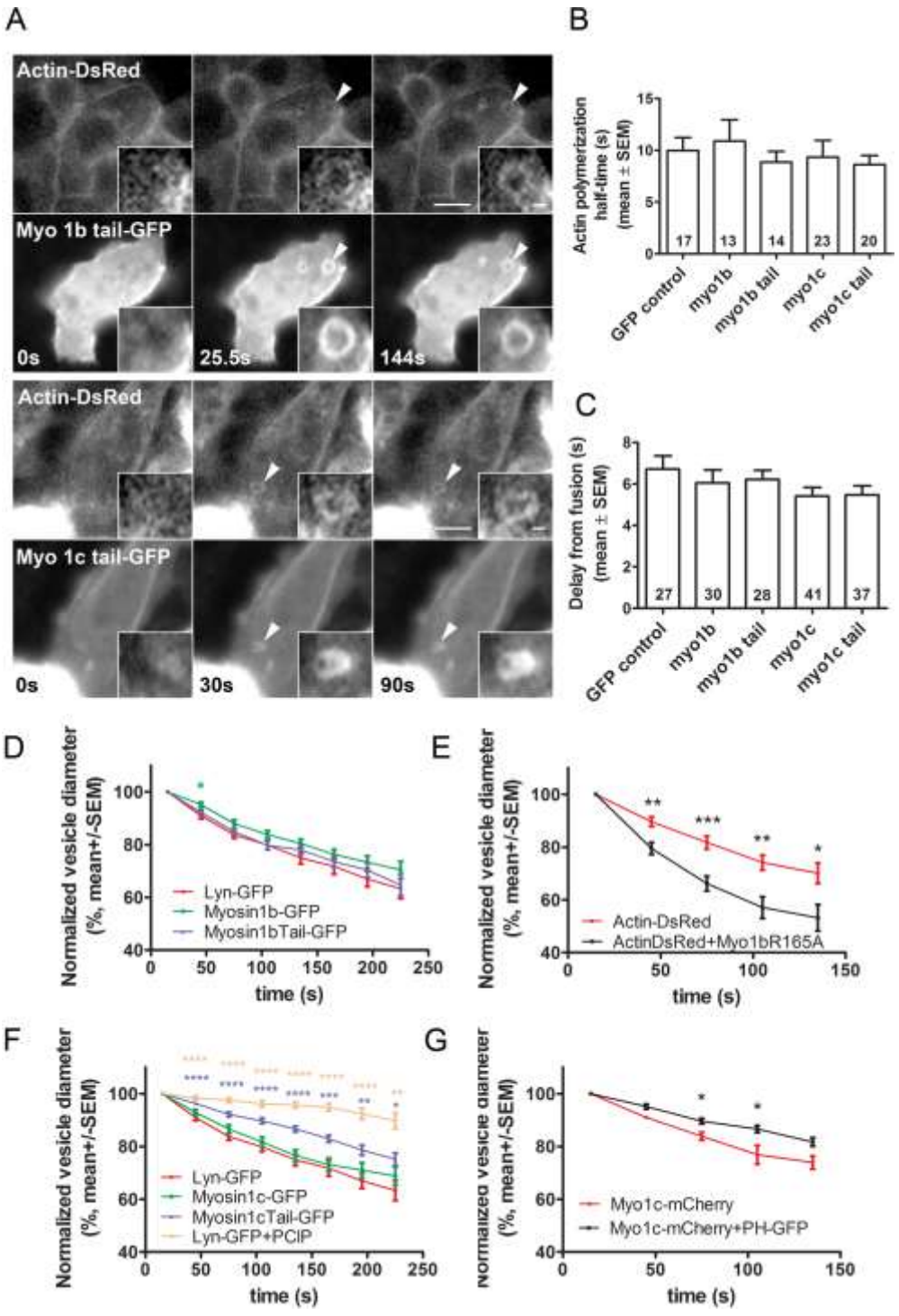

Figure 6: Actin coat formation and compression in ATII cells transfected with myosin 1b and myosin 1c constructs.

A) ATII cells co-transfected with actin-DsRed and myosin 1b tail-GFP (upper panel) or co-transfected with actin-DsRed and myosin 1c tail-GFP (lower panel). Myosin 1b tail-GFP and

myosin 1c tail-GFP translocated to fused secretory vesicles, which coated with actin. Time = 0 indicates the last time point before fusion, arrowheads point at the fusing vesicle and the inserts show the enlarged view of fusing LBs. Scale bars represent 10 µm (image) and 1 µm (insert).

B) Mean ± SEM of the half time for actin polymerization on fused vesicles in ATII cells transfected with actin-DsRed and co-transfected with GFP or GFP-tagged myosin 1b or myosin 1c constructs. Numbers indicate the number of actin coats. No significant difference of half times for actin polymerization could be observed between cells transfected with GFP control and myosin constructs (two-tailed Mann-Whitney test).

C) Mean ± SEM of the delay from the fusion pore opening to the start of actin coat formation in ATII cells transfected with actin-DsRed and co-transfected with GFP-tagged myosin 1b or myosin 1c constructs. Numbers indicate the number of actin coats. No significant difference of delay from fusion for actin polymerization could be observed between cells transfected with GFP control and myosin constructs (two-tailed Mann-Whitney test).

D) Normalized vesicle diameter decrease after fusion in ATII cells transfected with either lyn-GFP, myosin 1b-GFP or myosin 1b tail-GFP (n=18, 31, and 44, respectively). A slower compression rate was observed in cells transfected with full-length myosin 1b-GFP, compared to lyn-GFP. *$p<0.05$; two-tailed t-test.

E) Normalized vesicle diameter decrease after fusion in ATII cells transfected with actin-DsRed (control) or co-transfected with actin-DsRed and myosin 1b R165A-GFP. Fused vesicles in cells co-transfected with actin-DsRed and myosin 1b R165A-GFP (n=15) compressed significantly faster than control vesicles in cells transfected with actin Ds-Red alone (n=16; *$p<0.05$, **$p<0.01$, ***$p<0.001$; two-tailed t-test).

F) Normalized vesicle diameter decrease after fusion in ATII cells transfected with either lyn-GFP, myosin 1c-GFP, myosin 1c tail-GFP, or lyn-GFP treated with 10 µM PClP (n=18, 43, 34, and 12, respectively). Fused vesicles in cells transfected with myosin 1c tail-GFP or treated with 10 µM PClP inhibitor compressed significantly slower than vesicles in cells transfected with the control construct lyn-GFP (*$p<0.05$, **$p<0.01$, ***$p<0.01$, ****$p<0.0001$; two-tailed t-test).

G) Normalized vesicle diameter decrease after fusion in ATII cells transfected with myosin 1c-mCherry (n=54) and in cells co-transfected with myosin 1c-mCherry and PH-GFP (n=29). The vesicle compression was slower in cells co-transfected with myosin 1c-mCherry and PH-GFP, however, the differences were significant only at time points 75 s and 105s (*$p<0.05$; two-tailed t-test).

References

Almeida, C. G., Yamada, A., Tenza, D., Louvard, D., Raposo, G. and Coudrier, E. (2011). Myosin 1b promotes the formation of post-Golgi carriers by regulating actin assembly and membrane remodelling at the trans-Golgi network. *Nat. Cell Biol.* **13**, 779–789.

Barylko, B., Jung, G. and Albanesi, J. P. (2005). Structure, function, and regulation of myosin 1C. *Acta Biochim. Pol.* **52**, 373–380.

Boguslavsky, S., Chiu, T., Foley, K. P., Osorio-Fuentealba, C., Antonescu, C. N., Bayer, K. U., Bilan, P. J. and Klip, A. (2012). Myo1c binding to submembrane actin mediates insulin-induced tethering of GLUT4 vesicles. *Mol. Biol. Cell* **23**, 4065–4078.

Bond, L. M., Brandstaetter, H., Sellers, J. R., Kendrick-Jones, J. and Buss, F. (2011). Myosin Motor Proteins are Involved in the Final Stages of the Secretory Pathways. *Biochem Soc Trans* **39**, 1115–1119.

Bose, A., Guilherme, A., Robida, S. I., Nicoloro, S. M. C., Zhou, Q. L., Jiang, Z. Y., Pomerleau, D. P. and Czech, M. P. (2002). Glucose transporter recycling in response to insulin is facilitated by myosin Myo1c. *Nature* **420**, 821–824.

Bose, A., Robida, S., Furcinitti, P. S., Chawla, A., Fogarty, K., Corvera, S. and Czech, M. P. (2004). Unconventional myosin Myo1c promotes membrane fusion in a regulated exocytic pathway. *Mol. Cell. Biol.* **24**, 5447–5458.

Brandstaetter, H., Kendrick-Jones, J. and Buss, F. (2012). Myo1c regulates lipid raft recycling to control cell spreading, migration and Salmonella invasion. *J. Cell Sci.* **125**, 1991–2003.

Cai, Z., Jitkaew, S., Zhao, J., Chiang, H.-C., Choksi, S., Liu, J., Ward, Y., Wu, L.-G. and Liu, Z.-G. (2013). Plasma membrane translocation of trimerized MLKL protein is required for TNF-induced necroptosis. *Nat. Cell Biol.* **15**, 1–13.

Chen, X. W., Leto, D., Chiang, S. H., Wang, Q. and Saltiel, A. R. (2007). Activation of RalA Is Required for Insulin-Stimulated Glut4 Trafficking to the Plasma Membrane via the Exocyst and the Motor Protein Myo1c. *Dev. Cell* **13**, 391–404.

Chinthalapudi, K., Taft, M. H., Martin, R., Heissler, S. M., Preller, M., Hartmann, F. K., Brandstaetter, H., Kendrick-Jones, J., Tsiavaliaris, G., Gutzeit, H. O., et al. (2011). Mechanism and Specificity of Pentachloropseudilin-mediated Inhibition of Myosin Motor Activity. *J. Biol. Chem.* **286**, 29700–29708.

Coudrier, E. and Almeida, C. G. (2011). Myosin 1 controls membrane shape by coupling F-Actin to membrane. *Bioarchitecture* **1**, 230–235.

Crawley, S. W., Mooseker, M. S. and Tyska, M. J. (2014). Shaping the intestinal brush border. *J. Cell Biol.* **207**, 441–451.

Cyr, J. L., Dumont, R. A. and Gillespie, P. G. (2002). Myosin-1c interacts with hair-cell receptors through its calmodulin-binding IQ domains. *J. Neurosci.* **22**, 2487–2495.

Czech, M. P. (2000). PIP2 and PIP3: complex roles at the cell surface. *Cell* **100**, 603–606.

Dietl, P. and Haller, T. (2005). Exocytosis of lung surfactant: from the secretory vesicle to the air-liquid interface. *Annu. Rev. Physiol.* **67**, 595–621.

Dietl, P., Frick, M., Mair, N., Bertocchi, C. and Haller, T. (2004). Pulmonary consequences of a deep breath revisited. *Biol. Neonate* **85**, 299–304.

Dietl, P., Liss, B., Felder, E., Miklavc, P. and Wirtz, H. (2010). Lamellar Body Exocytosis by Cell Stretch or Purinergic Stimulation: Possible Physiological Roles, Messengers and Mechanisms. *Cell. Physiol. Biochem.* **25**, 1–12.

Dietl, P., Haller, T. and Frick, M. (2012). Spatio-temporal aspects, pathways and actions of Ca(2+) in surfactant secreting pulmonary alveolar type II pneumocytes. *Cell Calcium* **52**, 296–302.

Diglio, C. and Kikkawa, Y. (1977). The type II epithelial cells of the lung. IV. Adaption and behavior of isolated type II cells in culture. *Lab Invest* **37**, 622–31.

Dobbs, L., Gonzalez, R. and Williams, M. (1986). An improved method for isolating type II cells in high yield and purity. *Am Rev Respir Dis* **134**, 141–5.

Eitzen, G. (2003). Actin remodeling to facilitate membrane fusion. *Biochim. Biophys. Acta - Mol. Cell Res.* **1641**, 175–181.

Fan, Y., Eswarappa, S. M., Hitomi, M. and Fox, P. L. (2012). Myo1c facilitates G-actin transport to the leading edge of migrating endothelial cells. *J. Cell Biol.* **198**, 47–55.

Fang, Q. and Lindau, M. (2014). How Could SNARE Proteins Open a Fusion Pore? *Physiology (Bethesda).* **29**, 278–285.

Frick, M., Eschertzhuber, S., Haller, T., Mair, N. and Dietl, P. (2001). Secretion in alveolar type II cells at the interface of constitutive and regulated exocytosis. *Am.J.Respir.Cell Mol.Biol.* **25**, 306–315.

Frick, M., Schmidt, K. and Nichols, B. J. (2007). Modulation of Lateral Diffusion in the Plasma Membrane by Protein Density. *Curr. Biol.* **17**, 462–467.

Gillespie, P. G. and Cyr, J. L. (2004). Myosin-1c, the hair cell's adaptation motor. *Annu. Rev. Physiol.* **66**, 521–545.

Giner, D., Neco, P., Francés, M. D. M., López, I., Viniegra, S. and Gutiérrez, L. M. (2005). Real-time dynamics of the F-actin cytoskeleton during secretion from chromaffin cells. *J. Cell Sci.* **118**, 2871–2880.

Greenberg, M. and Ostap, E. (2013). Regulation and Control of Myosin-I by the Motor and Light Chain Binding Domains. *Trends Cell Biol.* **23**, 81–89.

Greenberg, M. J., Lin, T., Goldman, Y. E., Schuman, H. and Ostap, E. M. (2012). Myosin IC generates power over a range of loads via a new tension-sensing mechanism. *Proc. Natl. Acad. Sci.* **109**, E2433–E2440.

Haller, T., Ortmayr, J., Friedrich, F., Volkl, H. and Dietl, P. (1998). Dynamics of surfactant release in alveolar type II cells. *Proc.Natl.Acad.Sci.U.S.A* **95**, 1579–1584.

Hokanson, D. E. and Ostap, E. M. (2006). Myo1c binds tightly and specifically to phosphatidylinositol 4,5-bisphosphate and inositol 1,4,5-trisphosphate. *Proc. Natl. Acad. Sci. U. S. A.* **103**, 3118–3123.

Hokanson, D. E., Laakso, J. M., Lin, T., Sept, D. and Ostap, E. M. (2006). Myo1c binds phosphoinositides through a putative pleckstrin homology domain. *Mol. Biol. Cell* **17**, 4856–4865.

Jahn, R. and Fasshauer, D. (2012). Molecular machines governing exocytosis of synaptic vesicles. *Nature* **490**, 201–207.

Komaba, S. and Coluccio, L. M. (2010). Localization of myosin 1b to actin protrusions requires phosphoinositide binding. *J. Biol. Chem.* **285**, 27686–27693.

Kovárová, M., Tolar, P., Arudchandran, R., Dráberová, L., Rivera, J. and Dráber, P. (2001). Structure-Function Analysis of Lyn Kinase Association with Lipid Rafts and Initiation of Early Signaling Events after Fcε Receptor I Aggregation. *Mol. Cell. Biol.* **21**, 8318–8328.

Laakso, J. M., Lewis, J. H., Shuman, H. and Ostap, E. M. (2008). Myosin I can act as a molecular force sensor. *Science (80-.).* **321**, 133–136.

Laakso, J. M., Lewis, J. H., Shuman, H. and Ostap, E. M. (2010). Control of myosin-I force sensing by alternative splicing. *Proc. Natl. Acad. Sci. U. S. A.* **107**, 698–702.

Lin, T., Tang, N. and Ostap, E. M. (2005). Biochemical and motile properties of Myo1b splice isoform. *J. Biol. Chem.* **280**, 41562–41567.

Malacombe, M., Bader, M.-F. and Gasman, S. (2006). Exocytosis in neuroendocrine cells: new tasks for actin. *Biochim. Biophys. Acta* **1763**, 1175–1183.

Manceva, S., Lin, T., Pham, H., Lewis, J. H., Goldman, Y. E. and Ostap, E. M. (2007). Calcium regulation of calmodulin binding to and dissociation from the myo1c regulatory domain. *Biochemistry* **46**, 11718–11726.

Martin, R., Jäger, A., Böhl, M., Richter, S., Fedorov, R., Manstein, D. J., Gutzeit, H. O. and Knölker, H.-J. (2009). Total synthesis of pentabromo- and pentachloropseudilin, and synthetic analogues--allosteric inhibitors of myosin ATPase. *Angew. Chem. Int. Ed. Engl.* **48**, 8042–8046.

Masedunskas, A., Sramkova, M., Parente, L., Sales, K. U., Amornphimoltham, P., Bugge, T. H. and Weigert, R. (2011). Role for the actomyosin complex in regulated exocytosis revealed by intravital microscopy. *Proc. Natl. Acad. Sci. U. S. A.* **108**, 13552–13557.

Mason, R. J. and Dobbs, L. G. (1980). Synthesis of phosphatidylcholine and phosphatidylglycerol by alveolar type II cells in primary culture. *J. Biol. Chem.* **255**, 5101–7.

Mazerik, J. N., Kraft, L. J., Kenworthy, A. K. and Tyska, M. J. (2014). Motor and tail homology 1 (TH1) domains antagonistically control myosin-1 dynamics. *Biophys. J.* **106**, 649–658.

McConnell, R. E. and Tyska, M. J. (2010). Leveraging the membrane - cytoskeleton interface with myosin-1. *Trends Cell Biol.* **20**, 418–426.

Miklavc, P., Wittekindt, O. H., Felder, E. and Dietl, P. (2009). Ca2+-dependent actin coating of lamellar bodies after exocytotic fusion: a prerequisite for content release or kiss-and-run. *Ann.N.Y.Acad.Sci.* **1152**, 43–52.

Miklavc, P., Frick, M., Wittekindt, O. H., Haller, T. and Dietl, P. (2010). Fusion-activated Ca(2+) entry: an "active zone" of elevated Ca(2+) during the postfusion stage of lamellar body exocytosis in rat type II pneumocytes. *PLoS.One.* **5**, e10982.

Miklavc, P., Mair, N., Wittekindt, O. H., Haller, T., Dietl, P., Felder, E., Timmler, M. and Frick, M. (2011). Fusion-activated Ca2+ entry via vesicular P2X4 receptors promotes fusion pore opening and exocytotic content release in pneumocytes. *Proc. Natl. Acad. Sci. U. S. A.* **108**, 14503–8.

Miklavc, P., Hecht, E., Hobi, N., Wittekindt, O. H., Dietl, P., Kranz, C. and Frick, M. (2012). Actin coating and compression of fused secretory vesicles are essential for surfactant secretion: a role for Rho, formins and myosin II. *J.Cell Sci.* **125**, 2765–2774.

Miklavc, P., Ehinger, K., Sultan, A., Felder, T., Paul, P., Gottschalk, K.-E. and Frick, M. (2015). Actin depolymerisation and crosslinking join forces with myosin II to contract actin coats on fused secretory vesicles. *J. Cell Sci.* **128**, 1193–1203.

Nemoto, T., Kojima, T., Oshima, A., Bito, H. and Kasai, H. (2004). Stabilization of exocytosis by dynamic F-actin coating of zymogen granules in pancreatic acini. *J. Biol. Chem.* **279**, 37544–37550.

Nightingale, T. D., White, I. J., Doyle, E. L., Turmaine, M., Harrison-Lavoie, K. J., Webb, K. F., Cramer, L. P. and Cutler, D. F. (2011). Actomyosin II contractility expels von Willebrand factor from Weibel-Palade bodies during exocytosis. *J. Cell Biol.* **194**, 613–629.

Nightingale, T. D., Cutler, D. F. and Cramer, L. P. (2012). Actin coats and rings promote regulated exocytosis. *Trends Cell Biol.* **22**, 329–37.

Papadopulos, A., Tomatis, V. M., Kasula, R. and Meunier, F. (2013). The Cortical Acto-Myosin Network: From Diffusion Barrier to Functional Gateway in the Transport of Neurosecretory Vesicles to the Plasma Membrane. *Front. Endocrinol. (Lausanne).* **4**, 153.

Porat-Shliom, N., Milberg, O., Masedunskas, A. and Weigert, R. (2012). Multiple roles for the actin cytoskeleton during regulated exocytosis. *Cell. Mol. Life Sci.* **70**, 2099–121.

Prosperi, M.-T., Lepine, P., Dingli, F., Paul-Gilloteaux, P., Martin, R., Loew, D., Knolker, H.-J. and Coudrier, E. (2015). Myosin 1b functions as an effector of EphB signaling to control cell repulsion. *J. Cell Biol.* **210**, 347–361.

Raposo, G., Cordonnier, M. N., Tenza, D., Menichi, B., Dürrbach, a, Louvard, D. and Coudrier, E. (1999). Association of myosin I alpha with endosomes and lysosomes in mammalian cells. *Mol. Biol. Cell* **10**, 1477–1494.

Ridsdale, R., Na, C.-L., Xu, Y., Greis, K. D. and Weaver, T. (2011). Comparative proteomic analysis of lung lamellar bodies and lysosome-related organelles. *PLoS One* **6**, e16482.

Rizo, J. and Südhof, T. C. (2012). The Membrane Fusion Enigma: SNAREs, Sec1/Munc18 Proteins, and Their Accomplices—Guilty as Charged? *Annu. Rev. Cell Dev. Biol.* **28**, 279–308.

Rojo Pulido, I., Nightingale, T. D., Darchen, F., Seabra, M. C., Cutler, D. F. and Gerke, V. (2011). Myosin Va acts in concert with Rab27a and MyRIP to regulate acute von-Willebrand factor release from endothelial cells. *Traffic* **12**, 1371–1382.

Rooney, S. A. (2001). Regulation of surfactant secretion. *Comp. Biochem. Physiol. A. Mol. Integr. Physiol.* **129**, 233–43.

Ruppert, C., Godel, J., Müller, R. T., Kroschewski, R., Reinhard, J. and Bähler, M. (1995). Localization of the rat myosin I molecules myr 1 and myr 2 and in vivo targeting of their tail domains. *J. Cell Sci.* **108 (Pt 1**, 3775–3786.

Salas-Cortes, L., Ye, F., Tenza, D., Wilhelm, C., Theos, A., Louvard, D., Raposo, G. and Coudrier, E. (2005). Myosin Ib modulates the morphology and the protein transport within multi-vesicular sorting endosomes. *J. Cell Sci.* **118**, 4823–4832.

Sarshad, A., Sadeghifar, F., Louvet, E., Mori, R., Böhm, S., Al-Muzzaini, B., Vintermist, A., Fomproix, N., Östlund, A. K. and Percipalle, P. (2013). Nuclear Myosin 1c Facilitates the Chromatin Modifications Required to Activate rRNA Gene Transcription and Cell Cycle Progression. *PLoS Genet.* **9**, 1–16.

Schmidt, K. and Nichols, B. J. (2004). A Barrier to Lateral Diffusion in the Cleavage Furrow of Dividing Mammalian Cells. *Curr. Biol.* **14**, 1002–1006.

Shimada, T., Sasaki, N., Ohkura, R. and Sutoh, K. (1997). Alanine scanning mutagenesis of the switch I region in the ATPase site of Dictyostelium discoideum myosin II. *Biochemistry* **36**, 14037–14043.

Shuman, H., Greenberg, M. J., Zwolak, A., Lin, T., Sindelar, C. V, Dominguez, R. and Ostap, E. M. (2014). A vertebrate myosin-I structure reveals unique insights into myosin mechanochemical tuning. *Proc. Natl. Acad. Sci. U. S. A.* **111**, 2116–21.

Sokac, A. M., Co, C., Taunton, J. and Bement, W. (2003). Cdc42-dependent actin polymerization during compensatory endocytosis in Xenopus eggs. *Nat. Cell Biol.* **5**, 727–732.

Sokac, A. M., Schietroma, C., Gundersen, C. B. and Bement, W. M. (2006). Myosin-1c couples assembling actin to membranes to drive compensatory endocytosis. *Dev. Cell* **11**, 629–640.

Stauffer, E. A., Scarborough, J. D., Hirono, M., Miller, E. D., Shah, K., Mercer, J. A., Holt, J. R. and Gillespie, P. G. (2005). Fast adaptation in vestibular hair cells requires Myosin-1c activity. *Neuron* **47**, 541–553.

Swanljung-Collins, H. and Collins, J. H. (1991). Ca2+ stimulates the Mg2+-ATPase activity of brush border myosin I with three or four calmodulin light chains but inhibits with less than two bound. *J. Biol. Chem.* **266**, 1312–1319.

Swanljung-Collins, H. and Collins, J. H. (1992). Phosphorylation of brush border myosin I by protein kinase C is regulated by Ca2+-stimulated binding of myosin I to phosphatidylserine concerted with calmodulin dissociation. *J. Biol. Chem.* **267**, 3445–3454.

Tang, N., Lin, T. and Michael Ostap, E. (2002). Dynamics of Myo1c (Myosin-IBeta) Lipid Binding and Dissociation. *J. Biol. Chem.* **277**, 42763–42768.

Thorn, P. (2009). New insights into the control of secretion. *Commun. Integr. Biol.* **2**, 315–7.

Toyoda, T., An, D., Witczak, C. A., Koh, H. J., Hirshman, M. F., Fujii, N. and Goodyear, L. J. (2011). Myo1c regulates glucose uptake in mouse skeletal muscle. *J. Biol. Chem.* **286**, 4133–4140.

Várnai, P. and Balla, T. (2007). Visualization and manipulation of phosphoinositide dynamics in live cells using engineered protein domains. *Pflugers Arch. Eur. J. Physiol.* **455**, 69–82.

Weixel, K. M., Edinger, R. S., Kester, L., Guerriero, C. J., Wang, H., Fang, L., Kleyman, T. R., Welling, P. A., Weisz, O. A. and Johnson, J. P. (2007). Phosphatidylinositol 4-phosphate 5-kinase reduces cell surface expression of the epithelial sodium channel (ENaC) in cultured collecting duct cells. *J. Biol. Chem.* **282**, 36534–36542.

Woolner, S. and Bement, W. M. (2009). Unconventional myosins acting unconventionally. *Trends Cell Biol.* **19**, 245–252.

Yu, H.-Y. E. and Bement, W. M. (2007). Multiple myosins are required to coordinate actin assembly with coat compression during compensatory endocytosis. *Mol. Biol. Cell* **18**, 4096–4105.

Zeng, W. Z., Li, X. J., Hilgemann, D. W. and Huang, C. L. (2003). Protein kinase C inhibits ROMK1 channel activity via a phosphatidylinositol 4,5-bisphosphate-dependent mechanism. *J. Biol. Chem.* **278**, 16852–16856.

Zhu, T., Sata, M. and Ikebe, M. (1996). Functional expression of mammalian myosin I beta: analysis of its motor activity. *Biochemistry* **35**, 513–522.